Published in final edited form as:

Leukemia. 2022 August ; 36(8): 2009–2021. doi:10.1038/s41375-022-01614-0.

Novel mitochondria-targeting compounds selectively kill human leukemia cells

Svetlana B. Panina[*,1], **Jingqi Pei**[*,1], **Natalia Baran**[*,2], **Elissa Tjahjono**[1], **Shraddha Patel**[2], **Gheath Alatrash**[3], **Sergej N. Konoplev**[4], **Leonid A. Stolbov**[5], **Vladimir V. Poroikov**[5], **Marina Konopleva**[2], **Natalia V. Kirienko**[1,#]

[1]Department of BioSciences, Rice University, Houston, Texas, USA

[2]Department of Leukemia, The University of Texas MD Anderson Cancer Center, Houston, Texas, USA

[3]Department of Stem Cell Transplantation and Cellular Therapy, The University of Texas MD Anderson Cancer Center, Houston, Texas, USA

[4]Department of Hematopathology, The University of Texas MD Anderson Cancer Center, Houston, Texas, USA

[5]Institute of Biomedical Chemistry, Moscow, Russia

Abstract

Acute myeloid leukemia (AML) is a heterogeneous group of aggressive hematological malignancies commonly associated with treatment resistance, high risk of relapse, and mitochondrial dysregulation. We identified six mitochondria-affecting compounds (PS compounds) that exhibit selective cytotoxicity against AML cells *in vitro*. Structure-activity relationship studies identified six analogs from two original scaffolds that had over an order of magnitude difference between LD50 in AML and healthy peripheral blood mononuclear cells. Mechanistically, all hit compounds reduced ATP and selectively impaired both basal and ATP-linked oxygen consumption in leukemic cells. Compounds derived from PS127 significantly upregulated production of reactive oxygen species (ROS) in AML cells and triggered ferroptotic, necroptotic, and/or apoptotic cell death in AML cell lines and refractory/relapsed AML primary samples. These compounds exhibited synergy with several anti-leukemia agents in AML, acute lymphoblastic leukemia (ALL), or chronic myelogenous leukemia (CML). Pilot *in vivo* efficacy studies indicate anti-leukemic efficacy in a MOLM14/GFP/LUC xenograft model, including

[#]Correspondence: kirienko@rice.edu.
[*]These authors contributed equally to this work

Author Contributions

SBP and JP performed the majority of the experiments and wrote the first draft of the manuscript. NB assisted with ATP measurements, conducted seahorse experiments, flow cytometry experiments, mouse studies, and contributed to manuscript writing and editing. ET performed some of the experiments and contributed to manuscript writing and editing. SP assisted with mouse experiments and provided patient samples, GA, and SNK provided healthy bone marrow and patient samples. LAS and VVP performed cheminformatic analysis. MK and NK performed overall design of the study, acquired funding, and contributed to data analysis and manuscript writing and editing. All authors reviewed the manuscript before submission.

Competing interests

The authors have declared that no competing interests exist.

Code availability

The code that supports the findings of this study are available from the corresponding author upon reasonable request.

extended survival in mice injected with leukemic cells pre-treated with PS127B or PS127E and in mice treated with PS127E at a dose of 5 mg/kg. These compounds are promising leads for development of future combinatorial therapeutic approaches for mitochondria-driven hematologic malignancies such as AML, ALL, and CML.

Introduction

The notion of the Warburg effect, while useful, has led cancer researchers to overlook the importance of mitochondrial metabolism in cancer. Recent reports have illuminated key roles for mitochondria; cancer cells show increased dependence on mitochondrial reactive oxygen species (ROS) and α-ketoglutarate production and demonstrate increased mitochondrial dependence on glucose and glutamine for survival (1, 2). Depriving tumor cells of these substances rapidly kills them, which led to the initial suggestions of the potential for targeting mitochondria for anti-cancer therapies (3, 4).

Recent studies have shown diverse mitochondrial abnormalities during AML tumorigenesis (reviewed in (5, 6)). Drugs targeting various aspects of mitochondrial biology, including ROS production, the electron transport chain (ETC), or the mitochondrial permeability transition pore effectively kill tumor cells (7–10). Metabolic plasticity and altered mitochondrial metabolism are also considered promising “druggable” targets in the treatment of AML, a group of hematological malignancies characterized by uncontrolled clonal proliferation of immature myeloid progenitor cells in the bone marrow and peripheral blood (11). Current induction and consolidation treatments for AML are often too toxic for patients who are elderly or have comorbidities and have undesirable rates of resistance and relapse (12), highlighting the serious unmet need for new and improved treatments.

We previously demonstrated that AML cells exhibit a particular sensitivity to mitochondria-targeting compounds, including rotenone, cytarabine, etoposide, and ABT-199 (venetoclax), likely due to their low coupling efficiency. Combining these treatments with complementary, non-mitochondria-targeting drugs generally synergized AML-specific cytotoxicity, supporting this approach (13, 14).

Mitophagy (macroautophagic turnover of mitochondria) is a key mechanism for eliminating dysfunctional or damaged organelles and is crucial for cellular responses to physiological stresses (5, 15). The best-studied mechanism for mitophagic activation involves the PINK1 (PTEN-induced kinase 1)/Parkin axis, which licenses mitochondrial turnover (16), but interest in manipulating mitophagy to improve cancer therapy has been building for some time (15, 17). Mitochondria-targeted redox agents and drug regimens that contain ceramide induce mitophagy in breast cancer and AML cells, respectively, are other examples (18, 19).

Previously, we screened ~45,000 small molecules in *Caenorhabditis elegans* for their ability to increase PINK-1::GFP, an ortholog of human PINK1 (20). We identified 8 compounds, namely PS30, PS34, PS83, PS103, PS106, PS127, and PS134, whose treatment triggered events associated with mitophagy. We hypothesized that treating leukemia cells with these compounds would trigger selective cell death in AML cells due to their sensitivity to mitochondrial damage.

Here we demonstrate that most PS compounds and their chemical analogs were cytotoxic for MOLM-13 cells (an AML cell line containing an FTL3-ITD mutation). The five most effective PS leads also killed other AML, ALL, and CML cells, while displaying much lower toxicity for the healthy cell controls. The most effective compounds reduced ATP levels and selectively impaired basal and ATP-linked oxygen consumption in leukemic cells. Compounds from the PS127 family significantly increased ROS generation in AML cells, activating Nrf1 expression, and inducing ferroptotic and/or necroptotic cell death. PS30B moderately reduced mitochondrial mass and membrane potential in AML but not in healthy cells. PS127B and PS127E efficiently killed both leukemic blast and leukemic stem cells by inducing apoptosis. These compounds exhibited synergy when combined with conventional chemotherapeutics for leukemia with diverse mechanisms of action (21–23), or with the novel mitochondrial inhibitor IACS-010759. The combination of PS30B and doxorubicin also showed synergy in immortalized and primary cells. Finally, pilot *in vivo* studies conducted on mice implanted with PS compound-pretreated leukemic cells or mice treated with PS127E *in vivo* after engraftment showed an extension of overall survival. Taken together, these data support these leads' potential for chemical optimization and future therapeutic development.

Methods

Cytotoxicity screen in MOLM-13 cells

Chemical analogs (n = 35) of most promising AML-toxic PS compounds (n = 6/8) were identified and ordered from MolPort (https://www.molport.com). A full list of tested compounds is available as Supplementary Table 1.

Cell culturing and primary AML samples

Cell culture, peripheral blood and bone marrow collection, and cell isolation were performed as previously described (13, 14). Peripheral blood samples were collected from 29 patients with AML (n=15 for cytotoxicity (Supplementary Table 2), n=14 for flow cytometric evaluation of viability and apoptosis in AML bulk and AML LSC) during standard diagnostic procedures after informed consent was obtained in accordance with the Institutional Review Board regulations of MD Anderson Cancer Center.

Treatments and cytotoxicity assays

The stock solutions of all compounds were dissolved in DMSO and stored at −80 °C. A list of compounds can be found in Supplementary Methods 1. 3-methyladenine was prepared as fresh solution in test media immediately prior to use.

Cytotoxicity assays were performed with Hoechst 33342 and propidium iodide cell labeling as described (24). Details on cell treatment, doses, and treatment duration for all experiments are listed in Supplementary Methods 2.

Mitochondrial mass, membrane potential, and ROS evaluation

Mitochondrial mass and membrane potential were measured using a FACSCanto Flow Cytometer (Becton Dickinson, CA) as previously described (13, 14). ROS measurement was performed as described (13, 14).

ATP and bioenergetic measurements

ATP levels were measured in MOLM-13 and healthy PBMCs after 16 h treatment with compounds using a luminescent assay (CellTiter-Glo^{R} 2.0) and performed as previously described (13, 14). Real-time mitochondrial function was also assessed in these cells as previously described (13, 14).

Viability and apoptosis evaluation in primary AML and healthy bone marrow patient samples

Viability and apoptosis evaluation was performed as described in Supplementary Methods 3.

Western blots

Standard western blot procedures were performed. The primary antibodies used are listed in Supplementary Methods 4.

Animal studies

All experimental animal procedures were approved by MD Anderson Cancer Center's Institutional Animal Care and Use Committee. Experimental details are in Supplementary Methods 5.

Quantification and statistical analysis

Survival data were analyzed by fitting dose-response models in Bioconductor package 'drc', the lethal doses 50 (LD50) for each drug with their 95%-confidence intervals were calculated (25). Protein bands were quantified using ImageJ (https://imagej.nih.gov/ij/). Drug combination landscapes were visualized using Bioconductor package 'synergyfinder' (26). Statistical analyses were performed as previously described (13, 14). Sample sizes are listed in figure legends.

Results

PS compounds and their chemical analogs are selectively toxic against MOLM-13 cells

MOLM-13 cells were exposed to PS compounds or the solvent-control (DMSO) at 10 μM for 72 h. Cytotoxicity assays showed that six compounds (PS30, PS34, PS83, PS103, PS106, and PS127) decreased cell viability by at least 15% (Fig. 1A). LD50 values for MOLM-13 cells at 72 h were determined for these six compounds (Supplementary Table 3) and a group of commercially available analogs (Supplementary Table 1, Supplementary Table 4, Supplementary Fig. 1). Promisingly, five analogs from the PS127 structure family had LD50 values between ~200 nM – 1 μM.

For PS compounds with LD50 < 20 μM, cytotoxicity in PBMCs obtained from healthy donors was tested as above, except that the upper testing bound dose was increased to 100 μM. The selectivity ratio ($LD50_{PBMC}/LD50_{MOLM-13}$) was calculated to identify compounds with greater therapeutic promise. Some PS molecules, such as PS30, lacked apparent cytotoxicity in PBMCs even at 100 μM (>90% cells alive; Supplementary Table 4, Supplementary Fig. 2F, *right*).

To reduce the number of compounds for further testing, analogs with a selectivity index lower than 10 or $LD50_{MOLM-13} > 5$ μM were triaged, yielding six prioritized hits from two scaffolds (PS30B and PS127B, PS127B1, PS127E, PS127F, and PS127G, Supplementary Table 4, also see Supplementary Fig. 2). The derived LD50 dose for each compound was experimentally confirmed (Supplementary Table 4, Fig. 1B).

PS leads are effective in additional leukemic cell lines

Previously, we determined that leukemia cells are particularly sensitive to mitochondrial damage (13). To further probe the effect of the PS compounds, a panel of AML (MOLM-14, THP-1, MV-4;11, OCI-AML2), ALL (CCRF-CEM, MOLT-4, RS-4;11), and CML (KU812) cell lines was treated with a range of concentrations of the PS compounds (doxorubicin and cytarabine served as positive controls) for 72 h. Derivatives of the PS127 scaffold showed LD50 values ranging from 90 nM – 3 μM in all cell lines tested (Table 1). In contrast, although PS30B was generally effective against AML cells (LD50 ≤ 20 μM for 3 out of 4 cell lines), it had little effect on ALL or CML cells (Table 1). This suggests that the two compounds likely function through distinct mechanisms.

PS127 family compounds induce ROS

To study the effects of the selected PS compounds on mitochondria, MOLM-13 cells were exposed to compounds at LD50 at 72 h (150 nM rotenone was a positive control (27)) (Supplementary Fig. 3). ROS production was measured at 24 h to limit cell death. PS127 family analogs upregulated ROS, whether measured with dihydroethidium (DHE) or mitoSox (a mitochondria-targeted derivative of DHE) (Fig. 2A). Increased ROS production was specific to AML cells and was not observed in PBMCs, suggesting that this may be a determinant of cytotoxicity. This is consistent with our observations that ROS were not increased in either cell type after treatment with PS30B.

Next, we assessed changes in mitochondrial physiology after 24 h exposure to representative compounds (PS127B, PS127E, or PS30B) (Fig. 1C) or doxorubicin (positive control) (Fig. 2B). Treatment with PS30B resulted in a slight, but statistically significant, decrease in mitochondrial mass. This effect was specific to MOLM-13 cells; PBMCs showed no change in mitochondrial mass, even at a tenfold-higher dose of drug (Fig. 2B, *right*, Supplementary Fig. 4A). PS127B and PS127E had no apparent effect on mitochondrial mass.

The effect on mitochondria was also assessed by staining with JC-1, a readout for mitochondrial membrane potential (MMP) (28). PS30B reduced MMP in MOLM-13 cells, but not in healthy PBMCs (Fig. 2C, Supplementary Fig. 4B). The proton gradient and MMP are thought to regulate ROS production through a feedback loop, where the leak of protons back down the gradient decreases the production of ROS (29). One possible explanation for

the lack of ROS production by PS30B is that the slight depolarization of the mitochondrial membrane may be limiting ROS generation.

PS127B and PS127E also upregulated expression of Nrf1 (Fig. 2D), a key regulator of mitochondrial biogenesis, proteasomal activity, and ROS-scavenging enzymes (30), consistent with the cells attempts to mitigate mitochondrial damage caused by these compounds.

PS molecules impair mitochondrial respiration in leukemic cells

Nrf1 also regulates certain aspects of the ETC (31). Given our previous findings regarding the importance of the ETC in AML, we examined the effect of these compounds on the ETC in the MOLM-13 cells. Steady-state levels of ATP were measured at 72 h. Each compound significantly reduced ATP at ½ LD50 when normalized for cell viability (Fig. 2E). PS30B reduced ATP even at ¼ LD50 dose.

A Seahorse bioanalyzer was used to analyze mitochondrial function of MOLM-13 cells or PBMCs treated with PS127 group compounds, PS30B, or doxorubicin for 16 h (Fig. 3A, B, Supplementary Fig. 5C). Consistent with ATP measurements, each PS molecule significantly decreased basal respiration (reduced by 19–79%) and ATP-linked respiration (reduced by 20–80%). This effect was specific to MOLM-13 cells, as only PS127F showed a small effect on ATP-linked OCR in PBMCs (Fig. 3C, D, Supplementary Table 5). Interestingly, the proton leak previously observed in MOLM-13 cells (32), was strongly abrogated by treatment with the PS compounds (Supplementary Fig. 6A), suggesting that this trait is necessary for the survival of these cancer cells.

Extracellular acidification rate (ECAR) represents the combined activity of glycolysis and the citric acid cycle (i.e., non-oxidative phosphorylation mechanisms of ATP production) (33). Four of the six PS compounds reduced ECAR by 29–50% in leukemic cells (Supplementary Fig. 6B), suggesting that the cells were not compensating for mitochondrial damage by upregulating glycolysis.

Pair-wise correlation analysis showed that ATP level, normalized to DMSO, significantly correlated with normalized coupling efficiency ($r = 0.76$, $p = 0.047$), corroborating the importance of coupling efficiency to ATP production, and ATP-linked respiration ($r = 0.87$, $p = 0.011$). These correlations were specific to MOLM-13 cells (Fig. 3E, F) and indicate that PS hit compounds selectively impair mitochondrial bioenergetics in AML cells and that the increase in PINK1 is likely occurring via different methods.

PS127 family compounds activate mitophagy, ferroptosis and/or necroptosis

To determine which programmed cell death pathways were involved in compound-induced cytotoxicity, MOLM-13 or PBMCs were exposed to PS127B, PS127E, or PS30B at LD50 values for 72 h. Cells were also treated with specific inhibitors for apoptosis, autophagy, pyroptosis, ferroptosis, and necroptosis at concentrations chosen on the basis of preliminary assessments of cytotoxicity at 72 h (Supplementary Fig. 7A) and published studies (13, 34, 35).

Both ferroptotic inhibitors, Fer-1 and Lipr-1, and the necroptotic inhibitor Nec-1 significantly attenuated MOLM-13 cell death caused by PS127B and PS127E (Fig. 4A, B). Nec-1 also rescued healthy PBMCs after treatment with PS127B or PS127E; ferroptotic inhibitors increased PBMC survival following PS127E exposure (Fig. 4A, B). In contrast, PS30B cytotoxicity in MOLM-13 cells was unaffected by these inhibitors (Supplementary Fig. 7B).

Since ferroptosis is characterized by the accumulation of lethal levels of ROS-damaged lipids (35) and both PS127B and PS127E increased ROS production (Fig. 2A), the observation of reduced cytotoxicity after treatment with the ferroptotic inhibitors was consistent. Ferrous iron was depleted from the culture medium using deferoxamine (36). As anticipated, deferoxamine reduced PS127E-mediated MOLM-13 cell death (Fig. 4C). The addition of N-acetyl-L-cysteine (NAC), a ROS scavenger, significantly decreased ROS and PS compound-mediated cytotoxicity in MOLM-13 cells (Fig. 4D, E).

In contrast, the addition of the pan-caspase inhibitor ZVAD did not increase cell survival, possibly due to mild toxicity under these conditions. There was also an attenuation of AML cell death when PS127B was combined with the autophagic inhibitor 3-MA (Fig. 4A). We observed increased levels of the mitophagic markers NDP52 and BNIP3L/NIX (Fig. 4H) and the necroptotic markers RIP and RIP3 (Fig. 4I) after treatment with PS127E. Taken together, PS compounds induce different types of cell death, including ferroptosis, necroptosis, and autophagy.

PS compounds exhibit synergy with other anti-cancer chemotherapeutics

To assess whether PS molecules can synergize with existing anti-leukemic therapy, we analyzed their combination with a small panel of leukemia drugs (37). Anthracyclines (doxorubicin) intercalate into DNA, causing DNA damage during replication and triggering apoptosis (23). Cytarabine is a cytosine nucleoside analog that prevents DNA replication (38). IACS-010759 is a clinical-grade, small-molecule inhibitor of Complex I of the ETC reported to inhibit tumor growth in AML, B-ALL and T-ALL models (21, 39–41). 6-mercaptopurine (6-MP) is an FDA-approved antimetabolite known to block nucleotide anabolism and purine salvage and showed good efficacy for ALL and CML (22).

For initial synergy experiments, we used PS127B and PS30B. Four treatment combinations exhibited strong synergistic cytotoxicity in AML cells compared to PBMCs ($p<0.05$, Fig. 5). Importantly, this led to clear differences in survival between leukemic and healthy cells (Fig. 5A, B). Synergy was particularly evident when leukemic cells were resistant to one of the drugs (Fig. 5B, Supplementary Table 6).

Next, we compared efficiency and selectivity of PS compound combinations to cytarabine/doxorubicin (Fig. 5, Table 1). Although cytarabine/doxorubicin more effectively reduced viability in MOLM-13 cells compared to PBMCs, the mean maximum synergy score of cytarabine and doxorubicin was 13.40, while synergy scores were >20 for all PS compound combinations. Combining PS molecules with doxorubicin led to selectivity comparable to the clinical standard of cytarabine and doxorubicin (Supplementary Table 6).

To understand which cell death mechanism is associated with PS combinations' synergistic cytotoxicity, we paired PS127E with complementary drugs, as this compound showed higher effectiveness against MOLM-13 cells and triggered ferroptosis and necroptosis. As expected, the addition of Nec-1 significantly reduced cytotoxicity of PS127E alone or in combination with IACS-010759, indicating the activation of necroptosis in MOLM-13 (Supplementary Fig. 7C).

The combination of PS127E with IACS-010759 further increased ROS production in MOLM-13 (Fig. 4F). Excitingly, the addition of NAC reduced both ROS level and cytotoxicity (Fig. 4G). MOLM-13 cells treated with half LD50 for both PS127E and IACS-010759 showed similar effect, indicating that PS combinations' synergistic cytotoxicity is associated with mitochondrial ROS (Supplementary Fig. 7D, E). This observation stayed true for the combination of PS127E/doxorubicin (Supplementary Fig. 7F, G). Furthermore, the combination of PS127E/IACS induced mitophagy and necroptosis, although we did not observe an increase between single and combined treatments (Supplementary Fig. 8). Taken together, combinations of PS molecule with other anti-cancer chemotherapeutics induced redox imbalance, which may explain their synergistic cytotoxicity.

PS hit compounds are effective against primary AML cells alone and in combination with other anti-leukemic agents

While these data are promising, MOLM-13 cells may inaccurately represent the efficacy of these agents in primary AML cells. Therefore, we tested the most promising combinations (based on synergy and selectivity) in freshly isolated primary cells from AML patients. A small number of samples (n=4) were used to determine concentration ranges for the drugs (Supplementary Table 7). Additional patient samples (n=13) were then used to test 7 combinations that showed synergy in MOLM-13 cells: PS127B or PS127E with doxorubicin, IACS-010759, or 6-MP and PS30B with doxorubicin (Supplementary Table 8, Supplementary Fig. 9, Supplementary Fig. 10). Most primary samples were resistant to PS30B (LD50 > 20 μM) and anti-leukemia drugs at the concentrations tested, regardless of their mechanism. However, all patients' samples were sensitive to PS127B and PS127E. For example, 39 patient sample-treatment combinations were tested for PS127B (13 patients, each tested with PS127B combined with one of three other drugs). 38 had synergy scores >10, and the last sample had a synergy score of 9.81 (10 was the synergy cutoff). This indicates that drug combinations may be effective at concentrations where individual compounds had little to no apparent effect on healthy cells (Fig. 5C). Interestingly, while PS127B was equally effective against samples with *de novo* or secondary AML, PS127E was significantly more effective in *de novo* AML setting. This difference was particularly profound for PS127E with doxorubicin, where the average synergy for 6 patient samples with secondary AML was only 7.7, compared to 19.3 for *de novo* AML types. Combining PS30B with doxorubicin produced synergy in most patient samples (10 out of 13). Interestingly, this combination was ineffective in samples with a low percentage of blast cells (Supplementary Table 9).

PS hit compounds induce apoptosis in blast bulk and leukemic stem cells and extend survival in AML xenograft models

To investigate compounds' ability to selectively kill bulk leukemic cells and leukemic stem/progenitor cells (LSC) and to evaluate the therapeutic window towards hematopoietic stem cells (HSC), additional patient samples (n=14) (Supplementary Table 10) and freshly harvested healthy bone marrow (hBM) samples (n=3) were used to test PS127B and PS127E via flow cytometry (Supplementary Fig. 11, Supplementary Fig. 12). 5 μM PS127B, and 5 μM or 10 μM PS127E, significantly reduced viability of leukemia blasts, as compared to hBM cells (Fig. 6A). These effects were preserved for LSCs, with superior *in vitro* efficacy against AML LSC ($CD34^+$ $CD38^-$ or if $CD34^-$, $CD38^+$ $CD123^+$) than hBM HSC cells ($CD34^+$ $CD38^-$) (Fig. 6B, Supplementary Fig. 12).

Reduction of AML viability was associated with induction of apoptosis, as measured by Annexin V flow cytometry. Apoptosis was induced in all three conditions, with averages of 17% for PS127B, 22% for 5 μM PS127E and 59% for 10 μM PS127E in AML bulk cells (Fig. 6C). PS127E induced apoptosis in AML LSC, with averages of 23.4% at 5 μM and 62.3% at 10 μM, while hBM HSC were apparently unaffected under all conditions (Fig. 6D).

To investigate the cytotoxicity of PS127B and PS127E *in vivo*, a MOLM14/GFP/LUC cell xenograft model was utilized in NSG mice.

Since pharmacology of these compounds requires further optimization, we first studied whether pre-treatment of AML cells would delay leukemic progression in NSG mice. MOLM14/GFP/LUC cells were treated with DMSO, 5 μM PS127B, or 0.88 μM PS127E for 24 h, washed, and injected at 1×10^6/100μl into NSG mice, followed by biweekly bioluminescence intensity (BLI) monitoring (Fig. 7A). Pre-treatment of MOLM14/GFP/LUC cells with both agents contributed to delayed progression of these aggressive leukemias (Fig. 7B, C) and led to significant extension of the overall survival of leukemia-bearing NSG mice (Fig. 7D). We next tested efficacy of an oral administration of PS127E at a dose of 5mg/kg (Fig. 7E), which moderately reduced leukemia burden, delayed AML progression (Fig. 7F, G), and extended overall survival compared to control (Fig. 7H).

Taken together, PS127B and PS127E constitute two hit compounds with evidence of anti-leukemic activity in primary relapsed/refractory AML patient samples and show preliminary *in vivo* efficacy. Further pharmacodynamic studies of these promising compounds as monotherapy and combinatorial approaches are warranted.

Discussion

The dependency of leukemia cells on mitochondria has frequently been identified as an abnormality present in various AML subsets (42, 43). Our targeted cytotoxicity screen showed that several compounds that trigger PINK-1/PINK1 accumulation induced 50% death in MOLM-13 cells at sub-micromolar doses, including ~200 nM for PS127E, which was 23-fold lower than what was required to kill 50% of healthy PBMCs. Although doses required for eradication of patient-derived AML cells were generally higher (0.5–2.8 μM),

they were substantially decreased by combining PS compounds with other AML therapies, like doxorubicin or IACS-010759.

Testing showed that 5 of the 6 best leads were from the PS127 structural family. The availability of several chemotypes of PS127 made it possible to better determine which regions of the chemical scaffold are relevant for cytotoxicity. The use of PASS (**P**rediction of **A**ctivity **S**pectra for **S**ubstances) software, which estimates probability of various biological activities based on multilevel atomic neighborhood descriptors (44), for four PS127 derivatives indicated that the presence of a nitroethenyl group (e.g., in PS127B and PS127E) was necessary for their effects; compounds lacking this group (PS127H and PS127K) lacked efficacy against MOLM-13 cells (Supplementary Table 1, Supplementary Fig. 13). Several compounds were effective for ALL and CML as well, consistent with generic leukemic dependency on mitochondria.

AML-selective cytotoxicity of PS compounds resulted in ATP depletion and reduction in oxygen consumption rates. For PS127-family compounds, cytotoxicity was associated with severe oxidative stress and induction of ferroptotic, necroptotic, and/or apoptotic cell death pathways. Previous studies revealed that the β-nitrostyrene moiety activates caspase-dependent apoptosis (45, 46), consistent with our structural analysis of PS127 analogs.

Synergistic drug combinations can reduce side effects and help overcome tumor resistance by lowering treatment dosages (reducing off-target effects) while simultaneously diversifying therapeutic targets (47). Our results showed that synergy scores for PS127B were highest in primary AML cells *in vitro* when combined with the conventional cytotoxic agent doxorubicin (Supplementary Table 8). PS127E exhibited maximal synergy scores > 40, including in four different patient samples treated with PS127E and IACS-010759. These data highlight that PS127 analogs are highly active in drug combinations.

PS127B and PS30B drug combinations exhibited strong synergy in primary AML samples, in primary and secondary leukemias. Unlike primary *de novo* leukemia, secondary AML has evolved from previous myelodysplasia or developed after exposure to environmental or therapeutic toxins, and often presents resistance to multiple traditional chemotherapies used for treating primary AML (48, 49) (Supplementary Table 10 lists primary AML samples). The combination of PS30B with doxorubicin showed significantly greater synergy in AML samples with more than 30% leukemic blast cells (Fig. 5, Supplementary Table 2, Supplementary Table 9).

Targeting mitophagy as a therapeutic approach for AML is still exploratory; reports describing both inhibition and activation of mitophagy as potential therapeutic strategies have been published (50, 51). One possible explanation for these differing outcomes may reflect differences in baseline susceptibility of specific cancer cell types due to experimental conditions or specific somatic mutations contributing to tumor growth. For example, under hypoxic conditions that reflect the bone marrow microenvironment, AML blasts and LSCs rely heavily on mitophagy, particularly FIS1-mediated mitophagy, for survival (52). Chemically blocking autophagy can enhance apoptosis and decrease *in vivo* tumor burden in

this context (53). In line with this, high gene and protein expression levels of FIS1 in AML patient samples predict reduced chances of complete remission after induction therapy (54).

The opposite approach – activating mitophagy – has been shown to eradicate AML blasts *in vitro* and *in vivo* (55). FLT3-ITD mutations, commonly observed in AML, suppress ceramide production, which is necessary for mitophagy-dependent cell death. Inhibiting FLT3 using tyrosine kinase inhibitors (56) or LCL-461, a ceramide analog targeted to mitochondria, induced lethal mitophagy in AML blasts (55). Interestingly, although PS compounds activate mitophagy by different mechanisms, cell lines bearing the FLT3-ITD mutation (such as MOLM-13, MOLM-14, or MV-4;11) were generally more sensitive to the PS leads (Table 1).

We are not the first group to report a positive effect for PINK1 accumulation on cancer cell growth. B5G1, a derivative of the mitophagy-stimulating compound betulinic acid, also triggers PINK1 upregulation, mitophagy, and cancer cell death (57). Similarly, a folate-modified version of methyl-β-cyclodextran increases PINK1 expression, LC3-II conversion, and anti-tumor activity (58). Finally, BAY87–2243, an extensively modified piperazine that inhibits Complex I of the ETC, increased ROS production and induced PINK1-dependent mitophagy, which was then followed by necroptosis and ferroptosis, similar to what we observed in PS127-treated AML cells (59). Although each showed a benefit from increased PINK1, none of these leads were identified via high-throughput and/or targeted screens, but were serendipitous discoveries. This suggests that further exploration of PINK1 as potential therapeutic target is likely warranted.

Lead Contact and Materials Availability

Further information and requests for resources and reagents should be directed to and will be fulfilled by the Lead Contact, Natalia V. Kirienko (kirienko@rice.edu). This study did not generate new unique reagents.

Supplementary Material

Refer to Web version on PubMed Central for supplementary material.

Acknowledgments

The study was supported by the CPRIT grant RR150044 and NIH NIGMS grant R35GM129294 to NVK and NIH NCI grants R01CA231364 and P50CA100632 to MK. Computer-aided estimation of which regions of the chemical scaffold are relevant for cytotoxicity (L.A.S. and V.V.P.) was performed in the framework of the Russian Federation Fundamental Research Program for the long-term period for 2021–2030 (No. 122030100170-5).

Data availability statement

The data in this study that support the findings of this study are available from the corresponding author upon reasonable request.

References

1. Weinberg F, Hamanaka R, Wheaton WW, Weinberg S, Joseph J, Lopez M, et al. Mitochondrial metabolism and ROS generation are essential for Kras-mediated tumorigenicity. Proc Natl Acad Sci U S A. 2010;107(19):8788–93. [PubMed: 20421486]
2. Wise DR, Thompson CB. Glutamine addiction: a new therapeutic target in cancer. Trends Biochem Sci. 2010;35(8):427–33. [PubMed: 20570523]
3. Battogtokh G, Cho YY, Lee JY, Lee HS, Kang HC. Mitochondrial-Targeting Anticancer Agent Conjugates and Nanocarrier Systems for Cancer Treatment. Front Pharmacol. 2018;9:922. [PubMed: 30174604]
4. Neagu M, Constantin C, Popescu ID, Zipeto D, Tzanakakis G, Nikitovic D, et al. Inflammation and Metabolism in Cancer Cell-Mitochondria Key Player. Front Oncol. 2019;9:348. [PubMed: 31139559]
5. Macleod K. Mitophagy and Mitochondrial Dysfunction in Cancer. Annu Rev Cancer Biol. 2020;4:41–60.
6. Moro L Mitochondrial Dysfunction in Aging and Cancer. J Clin Med. 2019;8(11).
7. Zanotto-Filho A, Delgado-Cañedo A, Schröder R, Becker M, Klamt F, Moreira JC. The pharmacological NFkappaB inhibitors BAY117082 and MG132 induce cell arrest and apoptosis in leukemia cells through ROS-mitochondria pathway activation. Cancer Lett. 2010;288(2):192–203. [PubMed: 19646807]
8. Zunino SJ, Storms DH. Resveratrol-induced apoptosis is enhanced in acute lymphoblastic leukemia cells by modulation of the mitochondrial permeability transition pore. Cancer Lett. 2006;240(1):123–34. [PubMed: 16226372]
9. Baccelli I, Gareau Y, Lehnertz B, Gingras S, Spinella JF, Corneau S, et al. Mubritinib Targets the Electron Transport Chain Complex I and Reveals the Landscape of OXPHOS Dependency in Acute Myeloid Leukemia. Cancer Cell. 2019;36(1):84–99.e8. [PubMed: 31287994]
10. Sillar JR, Germon ZP, DeIuliis GN, Dun MD. The Role of Reactive Oxygen Species in Acute Myeloid Leukaemia. Int J Mol Sci. 2019;20(23).
11. Kreitz J, Schönfeld C, Seibert M, Stolp V, Alshamleh I, Oellerich T, et al. Metabolic Plasticity of Acute Myeloid Leukemia. Cells. 2019;8(8).
12. Döhner H, Estey EH, Amadori S, Appelbaum FR, Büchner T, Burnett AK, et al. Diagnosis and management of acute myeloid leukemia in adults: recommendations from an international expert panel, on behalf of the European LeukemiaNet. Blood. 2010;115(3):453–74. [PubMed: 19880497]
13. Panina SB, Baran N, Brasil da Costa FH, Konopleva M, Kirienko NV. A mechanism for increased sensitivity of acute myeloid leukemia to mitotoxic drugs. Cell Death Dis. 2019;10(8):617. [PubMed: 31409768]
14. Panina SB, Pei J, Baran N, Konopleva M, Kirienko NV. Utilizing Synergistic Potential of Mitochondria-Targeting Drugs for Leukemia Therapy. Front Oncol. 2020;10:435. [PubMed: 32318340]
15. Wang Y, Liu HH, Cao YT, Zhang LL, Huang F, Yi C. The Role of Mitochondrial Dynamics and Mitophagy in Carcinogenesis, Metastasis and Therapy. Front Cell Dev Biol. 2020;8:413. [PubMed: 32587855]
16. Vara-Perez M, Felipe-Abrio B, Agostinis P. Mitophagy in Cancer: A Tale of Adaptation. Cells. 2019;8(5).
17. Yan C, Li TS. Dual Role of Mitophagy in Cancer Drug Resistance. Anticancer Res. 2018;38(2):617–21. [PubMed: 29374684]
18. Biel TG, Rao VA. Mitochondrial dysfunction activates lysosomal-dependent mitophagy selectively in cancer cells. Oncotarget. 2018;9(1):995–1011. [PubMed: 29416672]
19. Morad SAF, MacDougall MR, Abdelmageed N, Kao LP, Feith DJ, Tan SF, et al. Pivotal role of mitophagy in response of acute myelogenous leukemia to a ceramide-tamoxifen-containing drug regimen. Exp Cell Res. 2019;381(2):256–64. [PubMed: 31112736]
20. Tjahjono E, Pei J, Revtovich AV, Liu T-JE, Swadi A, Hancu MC, et al. Mitochondria-Affecting Small Molecules Ameliorate Proteostasis Defects Associated with Neurodegenerative Disease Sci Rep. 2021;11(1):17733. [PubMed: 34489512]

21. Molina JR, Sun Y, Protopopova M, Gera S, Bandi M, Bristow C, et al. An inhibitor of oxidative phosphorylation exploits cancer vulnerability. Nat Med. 2018;24(7):1036–46. [PubMed: 29892070]
22. Bostrom B, Erdmann G. Cellular pharmacology of 6-mercaptopurine in acute lymphoblastic leukemia. Am J Pediatr Hematol Oncol. 1993;15(1):80–6. [PubMed: 8447563]
23. Tacar O, Sriamornsak P, Dass CR. Doxorubicin: an update on anticancer molecular action, toxicity and novel drug delivery systems. J Pharm Pharmacol. 2013;65(2):157–70. [PubMed: 23278683]
24. Pei J, Panina SB, Kirienko NV. An Automated Differential Nuclear Staining Assay for Accurate Determination of Mitocan Cytotoxicity. J Vis Exp. 2020(159).
25. Ritz C, Baty F, Streibig JC, Gerhard D. Dose-Response Analysis Using R. PLoS One. 2015;10(12):e0146021. [PubMed: 26717316]
26. Ianevski A, He L, Aittokallio T, Tang J. SynergyFinder: a web application for analyzing drug combination dose-response matrix data. Bioinformatics. 2017;33(15):2413–5. [PubMed: 28379339]
27. Li N, Ragheb K, Lawler G, Sturgis J, Rajwa B, Melendez JA, et al. Mitochondrial complex I inhibitor rotenone induces apoptosis through enhancing mitochondrial reactive oxygen species production. J Biol Chem. 2003;278(10):8516–25. [PubMed: 12496265]
28. Chaoui D, Faussat AM, Majdak P, Tang R, Perrot JY, Pasco S, et al. JC-1, a sensitive probe for a simultaneous detection of P-glycoprotein activity and apoptosis in leukemic cells. Cytometry B Clin Cytom. 2006;70(3):189–96. [PubMed: 16568474]
29. Brookes PS. Mitochondrial H(+) leak and ROS generation: an odd couple. Free Radic Biol Med. 2005;38(1):12–23. [PubMed: 15589367]
30. Kari E, Teppo HR, Haapasaari KM, Kuusisto MEL, Lemma A, Karihtala P, et al. Nuclear factor erythroid 2-related factors 1 and 2 are able to define the worst prognosis group among high-risk diffuse large B cell lymphomas treated with R-CHOEP. J Clin Pathol. 2019;72(4):316–21. [PubMed: 30755497]
31. Evans MJ, Scarpulla RC. NRF-1: a trans-activator of nuclear-encoded respiratory genes in animal cells. Genes Dev. 1990;4(6):1023–34. [PubMed: 2166701]
32. Vélez J, Hail N, Konopleva M, Zeng Z, Kojima K, Samudio I, et al. Mitochondrial uncoupling and the reprograming of intermediary metabolism in leukemia cells. Front Oncol. 2013;3:67. [PubMed: 23565503]
33. Mookerjee SA, Brand MD. Measurement and Analysis of Extracellular Acid Production to Determine Glycolytic Rate. J Vis Exp. 2015(106):e53464. [PubMed: 26709455]
34. Jantas D, Chwastek J, Grygier B, Lasoń W. Neuroprotective Effects of Necrostatin-1 Against Oxidative Stress-Induced Cell Damage: an Involvement of Cathepsin D Inhibition. Neurotox Res. 2020;37(3):525–42. [PubMed: 31960265]
35. Dixon SJ, Lemberg KM, Lamprecht MR, Skouta R, Zaitsev EM, Gleason CE, et al. Ferroptosis: an iron-dependent form of nonapoptotic cell death. Cell. 2012;149(5):1060–72. [PubMed: 22632970]
36. Yao X, Zhang Y, Hao J, Duan HQ, Zhao CX, Sun C, et al. Deferoxamine promotes recovery of traumatic spinal cord injury by inhibiting ferroptosis. Neural Regen Res. 2019;14(3):532–41. [PubMed: 30539824]
37. Dombret H, Gardin C. An update of current treatments for adult acute myeloid leukemia. Blood. 2016;127(1):53–61. [PubMed: 26660429]
38. Tamamyan G, Kadia T, Ravandi F, Borthakur G, Cortes J, Jabbour E, et al. Frontline treatment of acute myeloid leukemia in adults. Crit Rev Oncol Hematol. 2017;110:20–34. [PubMed: 28109402]
39. Han L, Cavazos A, Baran N, Zhang Q, Kuruvilla VM, Gay JP, et al. Mitochondrial Oxphos As Survival Mechanism of Minimal Residual AML Cells after Induction Chemotherapy : Survival Benefit By Complex I Inhibition with Iacs-010759. Blood. 2019;134(Supplement_1):5161.
40. Baran N, Lodi A, Sweeney SR, Renu P, Kuruvilla VM, Cavazos A, et al. Mitochondrial Complex I Inhibitor Iacs-010759 Reverses the NOTCH1-Driven Metabolic Reprogramming in T-ALL Via Blockade of Oxidative Phosphorylation: Synergy with Chemotherapy and Glutaminase Inhibition. Blood. 2018;132((Supplement_1)):4020.

41. Rytelewski M, Harutyunyan K, Baran N, Mallampati S, Zal M, Cavazos A, et al. Inhibition of Oxidative Phosphorylation Reverses Bone Marrow Hypoxia Visualized in Imageable Syngeneic B-ALL Mouse Model. Frontiers in oncology. 2020;10. [PubMed: 32047721]

42. Castelli G, Pelosi E, Testa U. Emerging Therapies for Acute Myelogenus Leukemia Patients Targeting Apoptosis and Mitochondrial Metabolism. Cancers (Basel). 2019;11(2).

43. Basak NP, Banerjee S. Mitochondrial dependency in progression of acute myeloid leukemia. Mitochondrion. 2015;21:41–8. [PubMed: 25640960]

44. Filimonov DA, Lagunin AA, Gloriozova TA, Rudik AV, Druzhilovskii DS, Pogodin PV, et al. Prediction of the Biological Activity Spectra of Organic Compounds Using the Pass Online Web Resource. Chemistry of Heterocyclic Compounds. 2014;50(3):444–57.

45. Bright SA, Byrne AJ, Vandenberghe E, Browne PV, Mcelligott AM, Meegan MJ, et al. Selected nitrostyrene compounds demonstrate potent activity in chronic lymphocytic leukaemia cells, including those with poor prognostic markers. Oncol Rep. 2019;41(5):3127–36. [PubMed: 30896840]

46. Wang YY, Chen YK, Hsu YL, Chiu WC, Tsai CH, Hu SC, et al. Synthetic β-nitrostyrene derivative CYT-Rx20 as inhibitor of oral cancer cell proliferation and tumor growth through glutathione suppression and reactive oxygen species induction. Head Neck. 2017;39(6):1055–64. [PubMed: 28346709]

47. Han K, Jeng EE, Hess GT, Morgens DW, Li A, Bassik MC. Synergistic drug combinations for cancer identified in a CRISPR screen for pairwise genetic interactions. Nat Biotechnol. 2017;35(5):463–74. [PubMed: 28319085]

48. Rowe JM. Therapy of secondary leukemia. Leukemia. 2002;16(4):748–50. [PubMed: 11960361]

49. Veelken H, Licht T, Lais A, Köhler G, Mertelsmann R, Schaefer HE, et al. Drug resistance of secondary acute myeloid leukemia with megakaryoblastic features and p190 BCR-ABL rearrangement. Leuk Res. 1998;22(11):1021–7. [PubMed: 9783805]

50. Kim EH, Sohn S, Kwon HJ, Kim SU, Kim MJ, Lee SJ, et al. Sodium selenite induces superoxide-mediated mitochondrial damage and subsequent autophagic cell death in malignant glioma cells. Cancer Res. 2007;67(13):6314–24. [PubMed: 17616690]

51. Yan C, Luo L, Guo CY, Goto S, Urata Y, Shao JH, et al. Doxorubicin-induced mitophagy contributes to drug resistance in cancer stem cells from HCT8 human colorectal cancer cells. Cancer Lett. 2017;388:34–42. [PubMed: 27913197]

52. Pei S, Minhajuddin M, Adane B, Khan N, Stevens BM, Mack SC, et al. AMPK/FIS1-Mediated Mitophagy Is Required for Self-Renewal of Human AML Stem Cells. Cell Stem Cell. 2018;23(1):86–100.e6. [PubMed: 29910151]

53. Fay HRS, Dykstra KM, Johnson M, Cronin TL, Lutgen-Dunckley L, Martens BL, et al. Mitophagy Plays a Key Role in the Anti-Leukemic Activity of Autophagy Inhibitors Under Hypoxia in Acute Myeloid Leukemia. Blood. 2019;134(1):1278.

54. Abo Elwafa R, Gamaleldin M, Ghallab O. The clinical and prognostic significance of FIS1, SPI1, PDCD7 and Ang2 expression levels in acute myeloid leukemia. Cancer Genet. 2019;233–234:84–95.

55. Dany M, Gencer S, Nganga R, Thomas RJ, Oleinik N, Baron KD, et al. Targeting FLT3-ITD signaling mediates ceramide-dependent mitophagy and attenuates drug resistance in AML. Blood. 2016;128(15):1944–58. [PubMed: 27540013]

56. Daver N, Schlenk RF, Russell NH, Levis MJ. Targeting FLT3 mutations in AML: review of current knowledge and evidence. Leukemia. 2019;33(2):299–312. [PubMed: 30651634]

57. Yao N, Wang C, Hu N, Li Y, Liu M, Lei Y, et al. Inhibition of PINK1/Parkin-dependent mitophagy sensitizes multidrug-resistant cancer cells to B5G1, a new betulinic acid analog. Cell Death Dis. 2019;10(3):232. [PubMed: 30850585]

58. Kameyama K, Motoyama K, Tanaka N, Yamashita Y, Higashi T, Arima H. Induction of mitophagy-mediated antitumor activity with folate-appended methyl-β-cyclodextrin. Int J Nanomedicine. 2017;12:3433–46. [PubMed: 28496320]

59. Basit F, van Oppen LM, Schöckel L, Bossenbroek HM, van Emst-de Vries SE, Hermeling JC, et al. Mitochondrial complex I inhibition triggers a mitophagy-dependent ROS increase leading

to necroptosis and ferroptosis in melanoma cells. Cell Death Dis. 2017;8(3):e2716. [PubMed: 28358377]

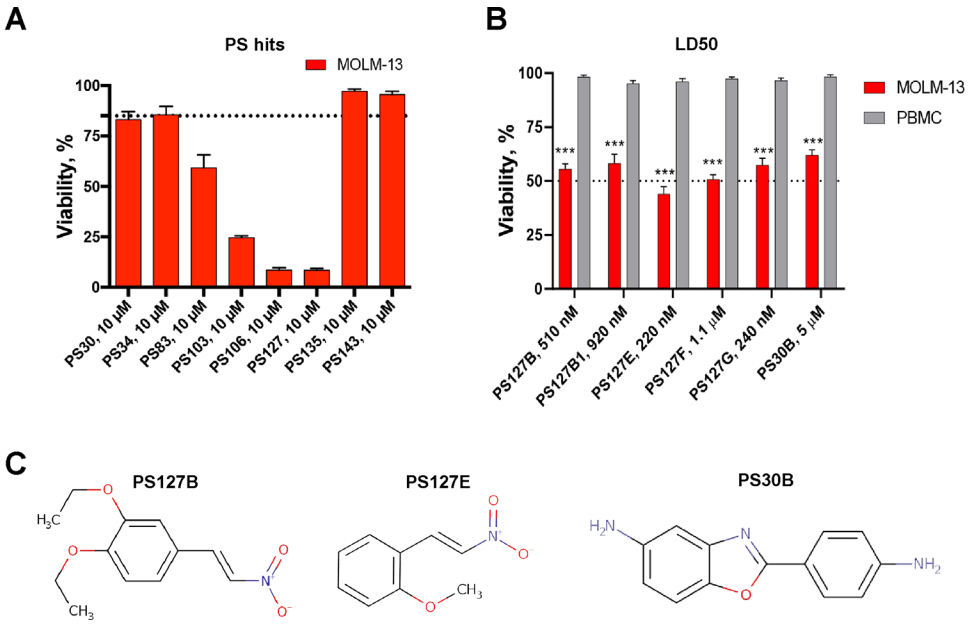

Fig. 1. Parental PINK-1 stabilizing (PS) compounds and their analogs as potential anti-AML agents.

A Cytotoxicity of parental PS compounds (n = 10, dose = 10 μM, 72 h treatment) against MOLM-13 cells. Cut-off survival (15%) is shown as a dotted line. **B** Experimental validation of fitted LD50 values for top leads. **C** Chemical structures of some leads. Bar graphs represent results (mean ± SEM) from at least three biological replicates **(A, B)**. Statistical testing was performed by multiple *t*-tests with independent samples: MOLM-13 vs PBMCs; ***$p < 0.001$.

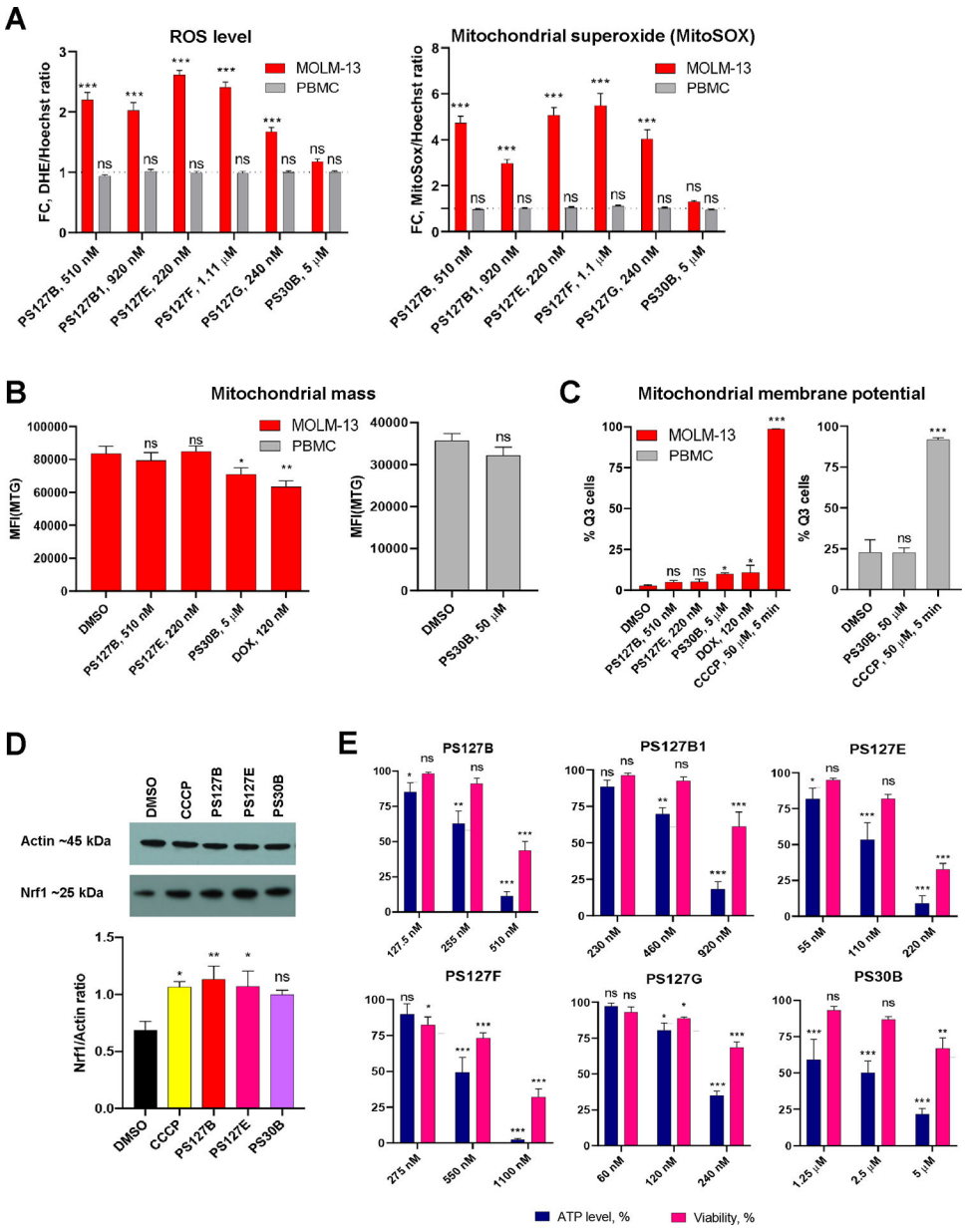

Fig. 2. Mitochondria-related mechanistic effects of PS hit compounds on cancer and normal blood cells.

A PS127 analogs, but not PS30B, increase cytosolic (*left*) and mitochondrial (*right*) ROS levels in leukemic cells (24 h). **B** PS30B compound decreases mitochondrial mass selectively in leukemic cells (24 h). Shown are mean fluorescence intensity (MFI) of Mitotracker Green (MTG) staining. **C** PS30B compound decreases mitochondrial membrane potential assayed by JC-1 staining in leukemic cells (24 h). Shown are % cells inside Q3 quadrant (representing cells with depolarized mitochondria). **D** Representative replicate (*top*) and quantification (*bottom*) of Nrf1 western blots. MOLM-13 cells were treated with LD50 of CCCP (2.5 μM), PS127B (510 nM), PS127E (220 nM), and PS30B (5 μM) for 24 h. Statistical testing vs DMSO **(A-D)** was performed by ANOVA with subsequent Dunnett's tests. **E** Changes of normalized ATP levels (in blue) and viability (in pink) of

MOLM-13 cells under treatment with PS leads (72 h). Statistical testing (ATP level & viability *vs*. control) was performed by ANOVA with subsequent Dunnett's tests. All bar graphs represent results (mean ± SEM) from at least three biological replicates. ***$p < 0.001$, **$p < 0.01$, *$p < 0.05$, ns – not significant.

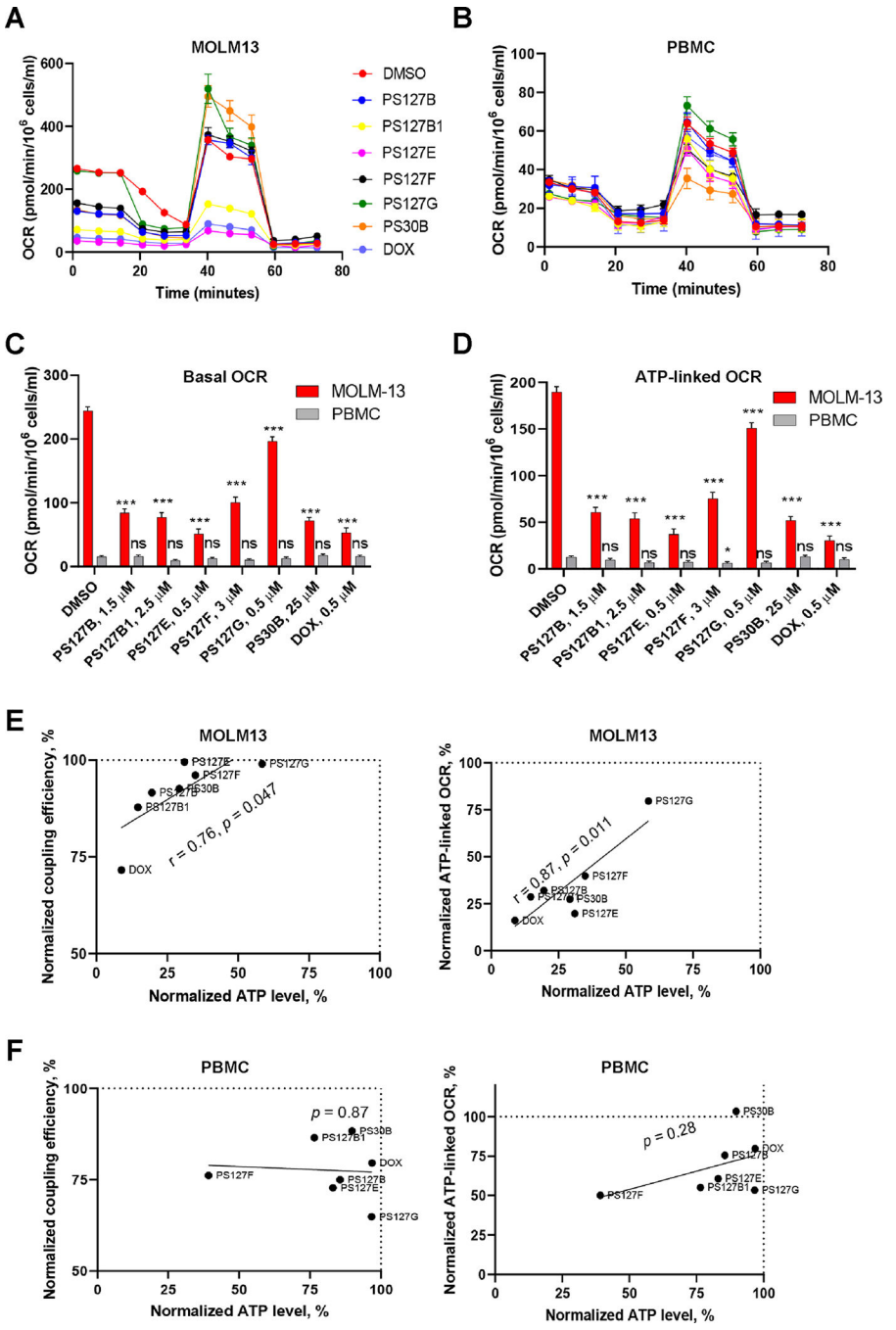

Fig. 3. Mitochondrial respiration in leukemic cells is selectively inhibited by PS leads.

A, B Representative OCR (oxygen consumption rate) curves of untreated cells (in red) and cells treated with PS compounds and doxorubicin (16 h) – MOLM-13 **(A)** and normal PBMCs **(B)**. **C, D** Changes in basal and ATP-linked respiration under PS compounds treatment in MOLM-13 cells (in red) and PBMCs (in grey) measured by Seahorse test. Statistical testing vs. DMSO was performed by ANOVA with subsequent Dunnet's tests; ***$p < 0.001$, *$p < 0.05$, ns – not significant. Bar graphs represent results (mean ± SEM) from at least three biological replicates. **E, F** Correlations between normalized ATP level

and Seahorse parameters (ATP-linked respiration, coupling efficiency) in MOLM-13 cells **(E)** and normal PBMCs **(F)**. Correlations were assessed between parameter averages from at least three biological replicates using Pierson's two-tailed correlation coefficient.

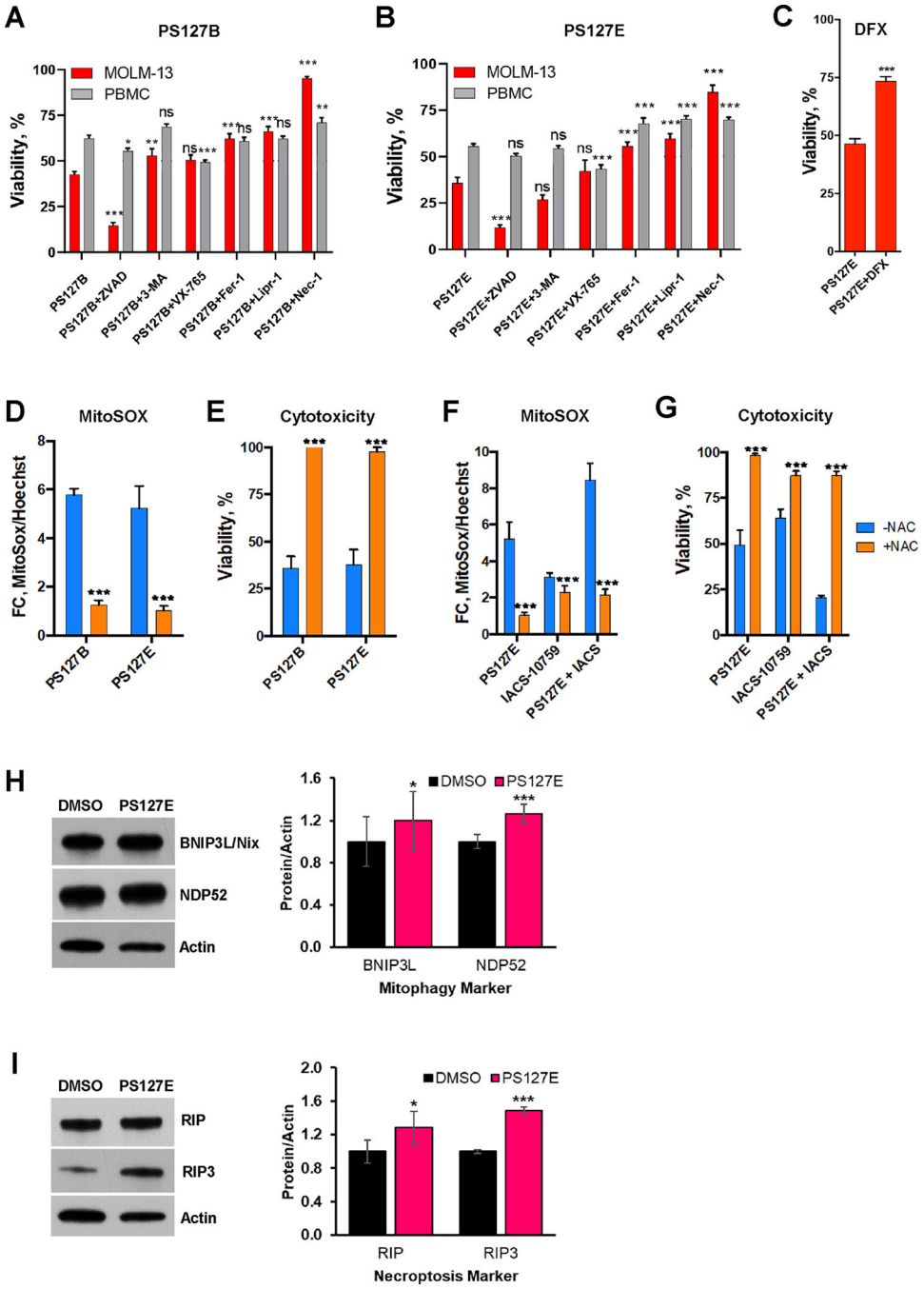

Fig. 4. PS molecules induce different cell death pathways.

A, B Survival rates of MOLM-13 cells (in red) and normal blood cells (in grey) under treatment with corresponding LD50 of PS127B (510 nM, 5.2 μM in MOLM-13, PBMCs, respectively); LD50 of PS127E (220 nM, 6 μM in MOLM-13, PBMCs, respectively) alone or in combination with cell death inhibitors (pan-caspase inhibitor Z-VAD-FMK (40 μM), 3-methyladenine (3-MA, 0.5 mM) as an inhibitor of autophagic cell death, the caspase-1 inhibitor VX-765 (10 μM), two ferroptotic inhibitors ferrostatin-1 (Fer-1, 0.5 μM) and liproxstatin-1 (Lipr-1, 0.5 μM), and the necroptotic inhibitor necrostatin-1 (Nec-1, 10 μM).

C Survival rate of MOLM-13 cells under treatment with PS127E (200 nM) alone or in combination with deferoxamine/DFX (40 μM). **D** Fold change of mitochondrial ROS level of MOLM-13 cells under treatment with PS127B or PS127E alone at LD50. **E** Normalized viability of MOLM-13 cells under treatment with PS127B or PS127E alone at LD50. **F** Fold change of mitochondrial ROS level of MOLM-13 cells under treatment with PS127E alone or in combination with IACS-010759 at LD50. **G** Normalized viability of MOLM-13 cells under treatment with PS127E alone or in combination with IACS-010759 at LD50. **H-I** Western blot of MOLM-13 cells treated with PS127E at LD50 for 24 h with **(H)** mitophagy markers NDP52 and BNIP3L/NIX or **(I)** necroptosis markers RIP and RIP3. Blots and quantifications were shown. Statistical testing vs corresponding LD50 value was performed by ANOVA with subsequent Dunnett's tests. All bar graphs represent results (mean ± SEM) from at least three biological replicates. *$p < 0.05$, **$p < 0.01$, ***$p < 0.001$, ns – not significant.

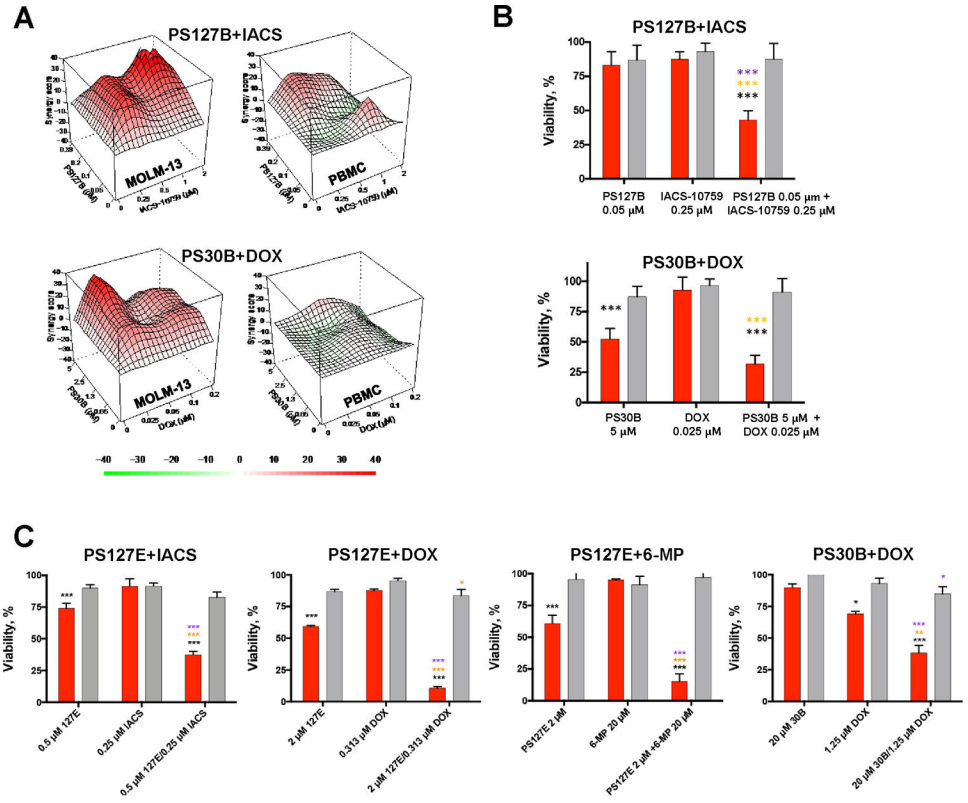

Fig. 5. PS compounds induced synergistic cytotoxicity when combined with other anti-cancer drugs in AML cell lines and primary AML samples.

A Representative synergy landscape and **B** cell survival rate under treatment with PS127B/PS30B along or in combinations with anti-cancer drugs (IACS-010759, DOX - doxorubicin) in MOLM-13 cells or PBMCs. **C** Comparison of viability under combinatorial treatment with PS compounds in a representative patient sample vs. PBMCs. Bar graphs represent results (mean ± SEM) from at least one biological replicate of a representative patient sample and three biological replicates of PBMCs. Significance of changes in survival was assessed via Student's t-test. $*p < 0.05$, $**p < 0.01$, $***p < 0.001$, ns – not significant. Black stars indicate comparison of AML cells vs. healthy PBMCs under the same treatment condition; purple stars indicate significantly lower survival under combinatorial treatment compared to single PS compounds; orange stars indicate significantly lower survival under combinatorial treatment compared to single complementary drug.

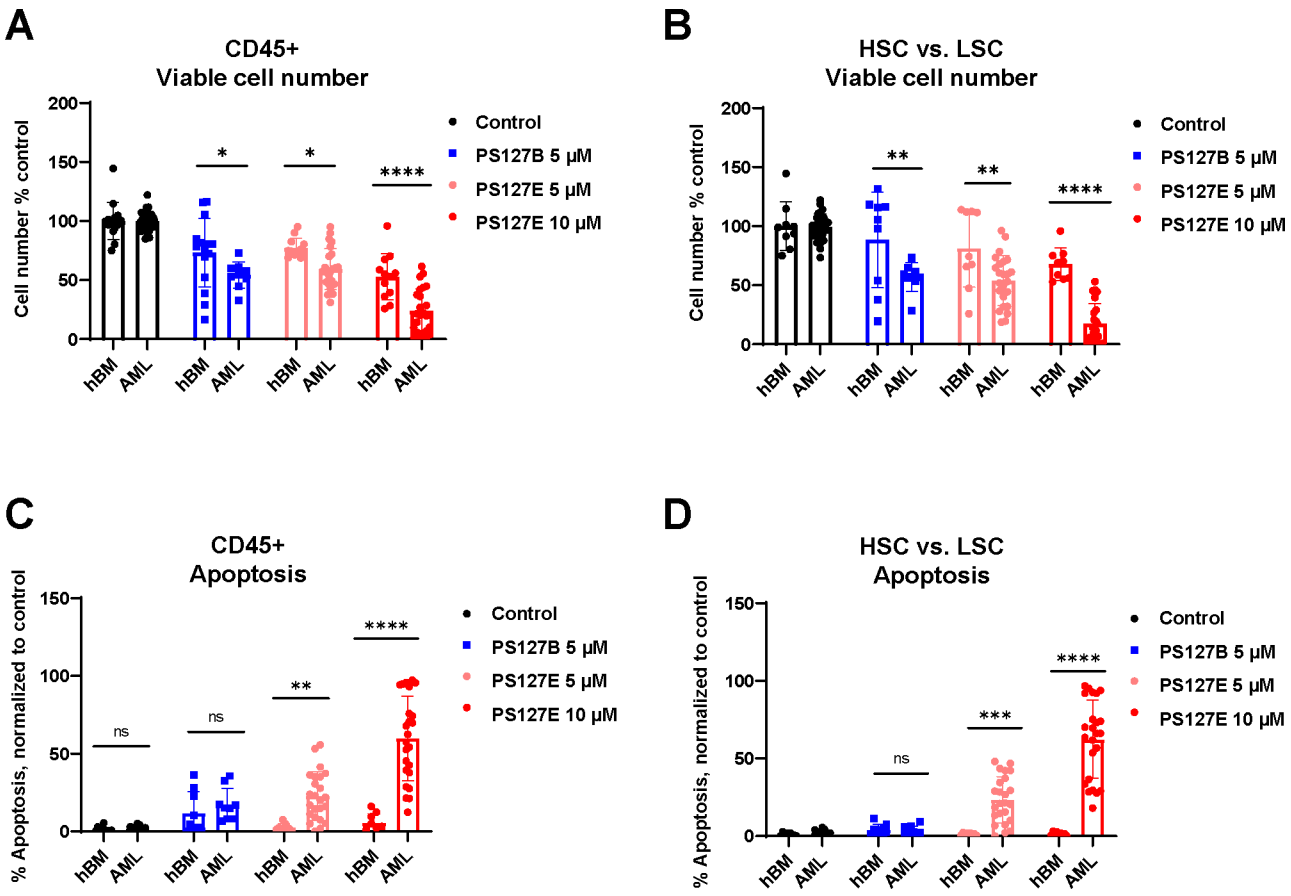

Fig. 6. Flow cytometry evaluation of viable cell number and apoptosis induction in primary AML samples and healthy bone marrow cells.

A Summary of viable cell number collected from CD45+ gate (Annexin V-/DAPI-), normalized to control, comparing response of AML (n=14) to that of hBM samples (n=3). **B** Summary of flow cytometric analysis of viable hematopoietic/leukemic stem cells gated by CD45+/CD34+/CD38− for HSC and CD45+/CD34+/CD38+ or CD38− for LSC (adjusted to clinical flow cytometry panel (Supplementary Table 10)). **C** Flow cytometric analysis of apoptotic cells collected from CD45+ gate (Annexin V+), normalized to control, comparing response to treatment in hBM samples (n=3) and leukemia patient samples (n=14). **D** Flow cytometric analysis of apoptotic hematopoietic/leukemic stem cells as gated by CD45+/CD34+/CD38− for HSC and CD45+/CD34+/CD38− or CD38+ or if negative for CD34+, then CD45+/CD38+/CD123+ for LSC (adjusted to clinical flow cytometry panel (Supplementary Table 10, Supplementary Fig. 12), normalized to control, comparing response to treatment in vitro of hBM samples (n=3) and leukemia patient samples (n=12). For panels (**A-D**) Data are shown as the mean ± SD; ns-p>0.5, *p < 0.05, **p < 0.01, ***p < 0.001, ****p < 0.0001.

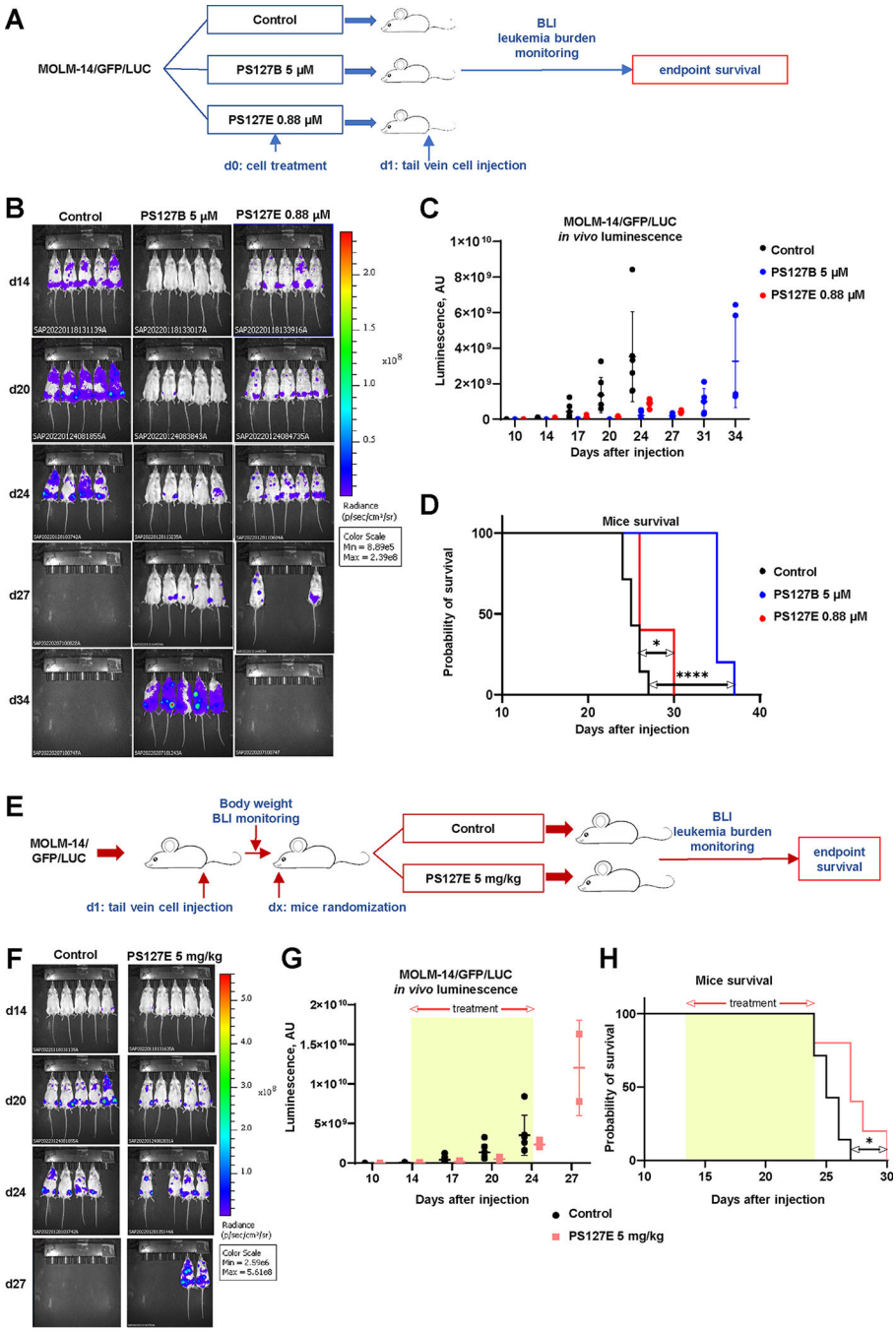

Fig. 7. Preclinical *in vivo* efficacy of PS127B and PS127E in MOLM14/GFP/LUC xenograft model.

A Schematics of the study addressing the efficacy of PS127B or PS127E pretreatment of MOLM14/GFP/LUC cells in NSG mice. MOLM14/GFP/LUC cells were pretreated with DMSO control, 5 μM PS127B, or 0.88 μM PS127E for 24 h. Cells were harvested and 1 million viable cells/100 μl was subjected to injection (n=5 mice per treatment condition). Monitoring of tumor burden was conducted by BLI. BLI measurement was obtained on day 1 and continued twice per week to monitor disease progression and overall survival. **B.**

Summary of leukemia burden progression in mice injected with cells treated with control, 5 μM PS127B, or 0.88 μM PS127E (dots represent separate mice). **C** Summary of BLI changes over time of mice in the study described in **(A). D** Kaplan-Meyer survival curve of mice injected with MOLM14/GFP/LUC cells pretreated with vehicle, 5 μM PS127B, or 0.88 μM PS127E. *$p < 0.05$; ****$p < 0.0001$. **E** Schematics of study addressing efficacy of PS127E in mice injected with MOLM14/GFP/LUC cells treated with DMSO or 5 mg/kg PS127E for 14 days (oral gavage, 5 days on, 2 days off). Mice' tumor burden was monitored by BLI; on day 14, mice were randomized and subjected to treatment with vehicle or 5mg/kg PS127E. Treatment timeframe is labeled with yellow window. For monitoring disease progression, BLI measurements were conducted on day 1 and then twice per week. **F** Summary of BLI changes over time in study described in **(E)**. **G** Summary of leukemia burden progression in mice injected with MOLM14/GFP/LUC cells treated with vehicle or 5 mg/kg PS127E. **H** Kaplan-Meyer survival curve of mice injected with MOLM14/GFP/LUC cells, treated with vehicle or 5mg/kg PS127E, *$p < 0.05$.

Table 1.

PS leads exhibit cytotoxicity against broad panel of AML, ALL, and CML cell lines.

Cell line	LD50 (95% CI), μM							
	PS127E	**PS127G**	**PS127B**	**PS127B1**	**PS127F**	**PS30B**	**DOX**	**ara-C**
Normal blood cells								
PBMCs	5.15 (4.01–6.29)	6.45 (4.57–8.32)	6.02 (5.23–6.80)	11.08 (9.73–12.43)	11.77 (8.82–14.71)	> 100	ND * (> 2.5 μM)	> 100
AML (acute myeloid leukemia)								
MOLM-13	0.22 (0.20–0.24)	0.24 (0.22–0.26)	0.51 (0.44–0.58)	0.92 (0.83–1.02)	1.11 (1.03–1.19)	4.96 (4.55–5.37)	0.12 (0.09–0.14)	0.015 (0.011–0.018)
MOLM-14	0.21 (0.16–0.27)	0.4 (0.35–0.46)	0.6 (0.58–0.62)	1.37 (1.21–1.53)	0.96 (0.93–0.99)	9.25 (8.16–10.33)	0.14 (0.12–0.16)	0.25 (0.23–0.28)
THP-1	0.36 (0.33–0.39)	0.51 (0.46–0.56)	1.1 (1.06–1.14)	1.25 (1.12–1.38)	2.68 (2.42–2.95)	20.04 (14.05–26.02)	0.41 (0.34–0.49)	0.82 (0.63–1.01)
MV-4;11	0.13 (0.12–0.14)	0.36 (0.30–0.42)	0.45 (0.42–0.48)	0.1 (0.89–1.11)	1.07 (0.90–1.24)	4.77 (4.10–5.43)	0.08 (0.07–0.10)	0.11 (0.10–0.13)
OCI-AML2	0.26 (0.21–0.31)	0.56 (0.46–0.65)	1.2 (1.02–1.39)	2.01 (1.61–2.42)	2.83 (2.35–3.31)	>20	0.3 (0.24–0.37)	0.1 (0.08–0.12)
ALL (acute lymphoblastic leukemia)								
CCRF-CEM	0.2 (0.18–0.22)	0.11 (0.08–0.14)	0.24 (0.21–0.26)	1.19 (1.13–1.25)	1.09 (1.02–1.15)	>20	3.66 (2.76–4.56)	2.48 (1.12–3.84)
MOLT-4	0.5 (0.47–0.52)	0.43 (0.39–0.46)	0.83 (0.78–0.86)	0.61 (0.57–0.65)	0.006 (0.004–0.008)	>20	0.018 (0.016–0.02)	0.0023 (0.0014–0.0032)
RS-4;11	0.09 (0.07–0.012)	0.47 (0.39–0.54)	1.07 (1.01–1.12)	1.93 (1.83–2.03)	3.01 (2.84–3.17)	>20	0.0073 (0.0060–0.086)	0.195 (0.12–0.27)
CML (chronic myelogenous leukemia)								
KU812	0.35 (0.30–0.40)	0.66 (0.62–0.71)	0.98 (0.88–1.07)	1.89 (1.74–2.05)	1.72 (1.65–1.79)	>20	0.096 (0.064–0.12)	>20

*ND, not defined. Doxorubicin (DOX) and cytarabine (ara-C) were included as controls. Cytotoxicity assay based on fluorescent Hoechst 33342-Propidium iodide double-staining does not allow the use of high doses of fluorescent compounds, like doxorubicin > 3 μM, as Hoechst signal is interfered by the fluorescent compounds.